THE JOURNAL OF PHYSICAL CHEMISTRY C

C: Physical Processes in Nanomaterials and Nanostructures

Adsorption of DNA Nitrogenous Bases on Nanodiamond Particles: Theory and Experiment

Kirill A. Laptinskiy, Ekaterina N. Vervald, Andrey N. Bokarev, Sergey A. Burikov, Marco D. Torelli, Olga A. Shenderova, Inna L. Plastun, and Tatiana A Dolenko

J. Phys. Chem. C, **Just Accepted Manuscript** • DOI: 10.1021/acs.jpcc.7b12618 • Publication Date (Web): 20 Apr 2018

ACS Publications

is published by the American Chemical Society. 1155 Sixteenth Street N.W., Washington, DC 20036

Adsorption of DNA Nitrogenous Bases on Nanodiamond Particles: Theory and Experiment

K.A. Laptinskiy[1], E.N. Vervald[1], A.N. Bokarev[2], S.A. Burikov[1], M.D. Torelli[3], O.A. Shenderova[3], I.L. Plastun[2], T.A. Dolenko[1]*

[1] *Department of Physics, Moscow State University, 119991 Moscow, Russia*

[2]*Department of Information Security of Automated Systems, Yuri Gagarin State Technical University of Saratov Politechnicheskaya str. 77, Saratov, Russia*

[3] *Adámas Nanotechnologies, Inc., 8100 Brownleigh Dr, Suit 120, Raleigh, NC, 27617 US*

**Corresponding author: laptinskij@physics.msu.ru*

Abstract

Efficiency of adsorption of nucleic acid nitrogenous bases on carboxylated detonation nanodiamond (DND-COOH) particles in aqueous media at pH=7.4-7.6 and pH=13.4 were investigated using Raman spectroscopy and infrared (IR) absorption spectroscopy. A significant difference in adsorption activity of nanodiamonds toward four different individual nitrogenous bases, guanine, adenine, cytosine and thymine) had been observed. The highest adsorption activity on DND-COOH was observed for cytosine and, in descending order, for adenine and thymine. At the same time, adsorption activity of the adenine-thymine and guanine-cytosine complementary pairs on nanodiamonds were similar. Analysis of the hydrogen bonds parameters

in adsorption of complementary pair adenine-thymine on nanodiamond surface had been done using the density functional theory based molecular modeling. The theoretical calculations are consistent with the experimental results.

Introduction

A large number of diseases, including infectious, cancer, and addictive disorders can benefit from genomic therapeutics.[1,2] One promising strategy to date to deliver genetic material is through nanoparticle-based transit, including nanoparticles composed of lipids, liposomes, polymers, and inorganic materials.[3-9] Immobilization of genetic material by nanocarriers provides shielding from the environment to overcome enzymatic degradation of the oligonucleotides, immunogenic responses, difficulty penetrating cells, off-target delivery, and clearance.[3-9] Among other inorganic nanocarriers, nanodiamond (ND) particles are a promising candidate as a general platform for genetic material delivery[9,10] due to its unique electrostatic surface profile and exceptional biological compatibility.[8-13]

ND's polyfunctional surface provides an opportunity for immobilization of large amounts of small and large molecules. Diamond has the highest known atomic density, which translates into the highest density of surface sites for drug loading. ND particles typically are polyfunctional, containing acidic, basic, and amphoteric surface groups simultaneously.[13] Carboxylation, reduction, and amination reactions produce different types of surface groups, but minority groups and small sp^2 carbon (hydrophobic) patches can still coexist.[12,13] Moreover, recent studies have shown the potential of NDs coated by cationic polymers as highly effective carriers for cell transfection with plasmid DNA,[14-18] siRNA,[14,15,19-22],and miRNA.[23] The efficiency of adsorption of linear versus circular strands of DNA had been studied in ref.[24] Strategies of direct attachment

of DNA to diamond surface have been demonstrated by various authors[25-30] including using thymidine as a linker,[25] through aromatic[28] and amid[29,30] bonds.

In the light of perspective of ND carriers in gene delivery, the elucidation of interaction mechanisms of DNA strands and oligonucleotides with the ND surface is required. In this work, we consider a simple model system consisting of individual DNA nitrogenous bases (NBs) (guanine (G), adenine (A), cytosine (C), thymine (T)). Besides one theoretical work[31] of the authors of this paper, we are not aware of experiments performed on adsorption of NBs on ND surface, while there is a wide array of experimental studies and theoretical calculations of the interactions of the individual NBs of DNA with carbon nanotubes,[32,33] the particles of graphite and graphene,[34-39] as well as particles of graphene oxide.[34]

It is known that hydrogen bonds play an important role in interactions of NDs surface groups with the surrounding molecules.[31,39-43] Detonation nanodiamonds (DND) dispersed in water weaken hydrogen bonds in water.[39-42] Moreover, the influence of DND on the strength of hydrogen bonds in solvent essentially depends on the surface functionalization of DND.[40,41] It was also found that, in its turn, the optical properties of DND depend on the strength of hydrogen bonds of the surface groups of the DND with the surrounding solvent molecules. Specifically, the stronger is hydrogen bonding between surface functional groups of DND and solvent molecules, the weaker are intrinsic fluorescent properties of DND.[41-43] These facts make it possible to consider DND as an efficient nano-agent in the biological tissue when using them as sensors or adsorbents of DNA.

This article presents the results of experimental and theoretical studies of non-covalent interactions of DNA NBs and DND. Using Raman spectroscopy and IR absorption spectroscopy the interactions between the carboxylated surface of DND and the nitrogenous bases of DNA in

water were studied. The comparative analysis of the adsorption activity of DND with respect to individual DNA NBs and their complementary pairs was performed. The process of adsorption of the complementary pairs of DNA NBs on the DND with COOH surface groups was numerically modeled. The mechanisms of adsorption were investigated experimentally and theoretically. The present study establishes a foundation for future applications of DND in the direction of biomedicine.

Experimental and Theoretical Methods

Materials and methods. Nanodiamonds preparation.

DND were synthesized by explosion of trinitrotoluene (TNT) and 1,3,5- trinitrotoluene-1,3,5-triazine (RDX) mixture in the media with water cooling (Real-Dzerzhinsk LTD, Russia). Samples were crushed in a planetary mill using zirconium beads. After crushing, the samples were purified in hydrochloric acid and heated in air for oxidation of non-diamond carbon and surface carboxylation. Centrifugal fractionation was carried out to obtain DND with size of 10 nm.

Suspensions of nanodiamond and DNA nitrogenous bases preparation.

DNA nitrogenous bases - adenine, guanine, thymine, cytosine, produced by SERVA (class “analytical grade”), were used in the experiments.

Deionized bidistilled water (with specific electrical conductivity 5 μS/m, pH=6.9) was used for preparation of NDs and NBs aqueous suspensions.

At pH = 7.4-7.6, the size of nanodiamonds in the aqueous suspension obtained by the DLS method is 10±1 nm, Zeta potential is -42±2 mV, specific surface area is $17.1 \cdot 10^{-2}$ m^2.[44]

Two experiments were carried out: (i) for aqueous solutions of A, T and C with the concentrations 1.03 g/L, 1.26 g/L and 1.11 g/L, accordingly; (ii) for aqueous solutions of A, T, C and G with the concentration 5 g/L. Value of pH was measured at the beginning and at the end of adsorption. In the experiment (i) the value of pH was changed from 7.4 - 7.6 up to 7.6 – 7.8, in the experiment (ii) – from 13.4 up to 13.8. Guanine was not used in the first set of experiments due to its very bad solubility in water at pH~7.4. Therefore, in the second experiment, alkali NaOH with concentration 0.5 M was added to all solutions in order to achieve the solubility of guanine.[45] In both experiments the initial concentration of DND in water was 2 g/L.

Experimental Characterization Setup.

Sizes of the particles in aqueous suspensions were measured by DLS method using the correlator-goniometric system ALV-CGS-5000/6010 (Langen, Germany), equipped with He-Ne laser (wavelength 632.8 nm, laser power 20 mW). For the computational processing of the obtained correlation functions the software package CONTIN was used.

Raman spectra were obtained using Raman spectrometer. For excitation of Raman signal the argon laser was used (wavelength 488 nm, operating power density 10 W/cm^2). The registration system consisted of monochromator (Acton, grade 900 grooves/mm, focal length 500 mm) and CCD-detector (Jobin Yvon, Syncerity BIUV). The spectral resolution was 2 cm^{-1}. The temperature of the samples was set and controlled by a thermostabilization system of with accuracy 0.2^{o}C.

Spectra of IR absorption of the samples were measured using a Varian 640-IR FT-IR spectrometer equipped with an attenuated total reflection cell with a ZnSe internal reflection element. The spectral resolution was 4 cm^{-1}.

Adsorption experiments.

To study an adsorption activity of DND-COOH toward to individual DNA NBs and their complementary pairs, the experiment was conducted as follows (Figure 1). Aqueous solutions of DNA NBs with known concentrations were added to initial DND aqueous suspension. In all samples the concentration of DND was the same. The values of pH and size distribution of nanoparticles were measured in mixtures–suspensions of NBs and DNDs. After several hours of incubation, supernatants and aggregates (adsorbate+adsorbent) were separated by centrifugation. The precipitate was washed several times with a solvent of corresponding pH. Then the values of pH and concentrations of DNA NBs in the supernatants were measured. In more details these experiments are described in the Supplementary Materials.

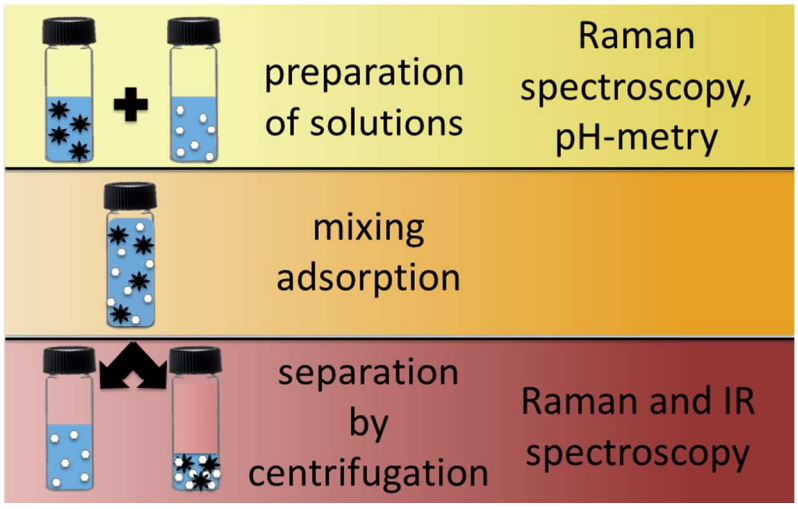

Figure 1. Scheme of experiment on the study of DND adsorption properties toward DNA NBs.

The NBs concentrations in the solutions (before and after adsorption) were determined using calibration curves of the dependence of intensity of their characteristic bands in the Raman spectrum on concentration. Figure 2 illustrates low-wavenumber regions of Raman spectra of A, T, G, C water solutions with concentration 5 g/L and characteristic bands chosen as markers of each NBs: adenine (704-771 cm^{-1}), thymine (742-804 cm^{-1}), cytosine (769-831 cm^{-1}), guanine (1255-1303 cm^{-1}).

First, the dependencies of intensity (defined as peak height) of each of specified marker of A, T and C on their concentration in water in the range from 0 to 1.03 g/L, 1.26 g/L and 1.11 g/L, accordingly, with concentration increment for A and T 0.13 g/L, for C – 0.11 g/L, were obtained. Then the dependencies of intensity of each of specified markers of A, T, C and G on their concentration in water in the range from 0 to 5 g/L with concentration increment 0.5 g/L were obtained. As in the other studies of the authors of this article,[46] it turned out that these dependencies are well-approximated by straight lines (Figure 3, Figures S1-S3). Moreover, the dependences of the intensities of the markers on the concentration of the corresponding NBs in water with/without addition of NaOH coincided in the relevant concentrations ranges of DNA NBs. One should note that the spectral lines of the markers, mentioned above, shift with the change of pH. Nevertheless, the maximum of the peak does not fall outside the mentioned in brackets range of wavenumbers. From the obtained calibration straight lines the concentration of each NB was determined. The error of concentration determination was 0.03 g/L for adenine, 0.05 g/L for guanine, 0.03 g/L for cytosine, 0.04 g/L for thymine.

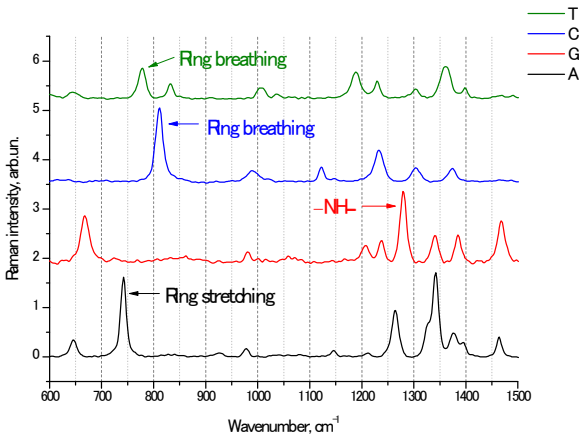

Figure 2 Low-wavenumber regions of DNA NBs aqueous solutions Raman spectra with concentration 5 g/L (pH=13.4).

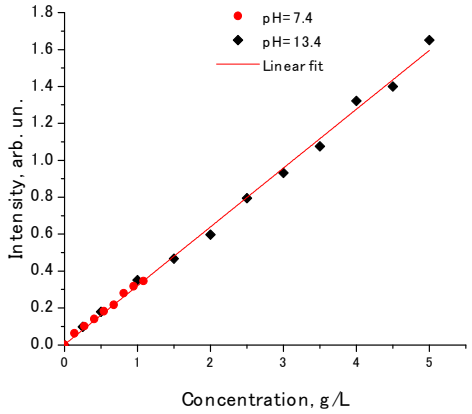

Figure 3. Calibration straight line of the dependence of adenine Raman marker intensity (704-771 cm^{-1}) on its concentration in aqueous solution. The error of adenine concentration determination was 0.03 g/L (0.22 mM).

The obtained calibration dependencies (Figure 3, Figures S1-S3) were used in experiments of DND adsorption toward both individual DNA NBs as well as their

complementary pairs for measuring the NBs concentration in suspensions before and after their adsorption on the DND surface.

Molecular Modeling Approach.

Modeling of structure and calculation of the molecular compounds spectra were performed by method of the density functional theory (DFT)[47] using the functional B3LYP[47,48] and the basis set 6-31G(d). In such basis set the atomic orbitals of the inner shell can be approximated by six Gaussian functions, M=6, and the orbitals of the valence shell can be described, respectively, by three (N=3) and one (P=1) Gaussian functions with addition of polarization components (taking into account the diffusion effects). In the calculations the software package Gaussian 09[49] was used. This software package is widely used for solution of molecular modelling problems in various fields of computational physics and chemistry.

In order to take into account anharmonicity in the interactions and to reduce the degree of divergence between the experimental and calculated data, consequently, the following scaling factors for the calculated frequencies were derived and used: 0.9713 (the region 0-1000 cm^{-1}); 0.9744 (the region 1000-2000 cm^{-1}); 0.956 (the region higher than 2000 cm^{-1}).

Results and Discussion

Adsorption of individual DNA nitrogenous bases on the nanodiamonds surface at physiological pH.

For the adsorption experiments at physiological pH DND-COOH aqueous suspensions with concentration 2 g/L were used with pH adjusted to 7.4–7.6. Average volumetric size of DND

particles was 10 nm according to DLS measurements. Aqueous solutions of adenine, thymine and cytosine were prepared at the following concentrations: A - 1.03 g/l, T – 1.26 g/L and C – 1.11 g/L at pH = 7.4–7.6. Guanine in water is poorly soluble[45] and was not used in this set of experiments.

For the control of NB concentration in the prepared solutions, Raman spectra were measured in the region from 600 to 1400 cm^{-1} (Figure 4). The NBs concentrations were confirmed using the calibration curves of characteristic Raman bands intensities.

The DND suspension was added to each NB solution in proportion 1:1. The mixtures were mixed with shaker Multi-Vortex V-32 (Biosan) during 2 hours followed by centrifugal separation of the supernatant (unbound NBs) and precipitate (DNDs with adsorbed NBs). In addition, the precipitate was flushed one more time in order to purify it from not adsorbed but simply precipitated NBs.

Raman spectra of the primary and secondary supernatants were measured in the region from 600 to 1400 cm^{-1} (Figures 4). The change of the concentration between initial solution and primary supernatant can be used to calculate the amount of NBs adsorbed on NDs surface. The absence of the spectral lines of NBs in secondary supernatant proves that nucleobases molecules are strongly adsorbed on NDs surface and that it did not precipitate by themselves. It should be noted that the shift of NB characteristic spectral bands on each stage of experiment was insignificant (less than 2 cm^{-1}). It could be indirect evidence of the absence of a destructive impact of DND on NB molecules.

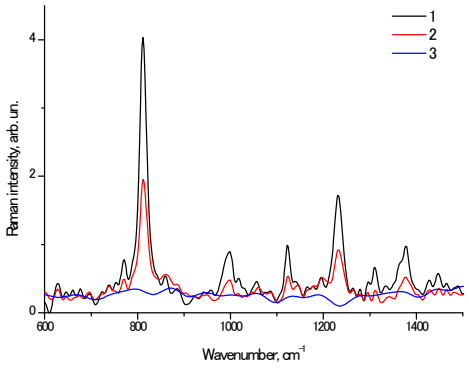

Figure 4. Low-wavenumber regions of Raman spectra of the initial solution (1), primary (2) and secondary (3) supernatants of cytosine.

The measurements of NBs concentrations in the initial mixtures and supernatants demonstrated that A, C and T are adsorbed to a different extent on the nanodiamond surface. The NBs concentrations in the supernatants were decreased after adsorption experiment relative to the initial concentrations as follows: A – by 18%, C – by 39%, T – by 8%.

The adsorption activity of DND toward each DNA NB was calculated. The adsorption activity is defined as the amount of adsorbed substance per unit of adsorbent surface area. The DND total surface area was calculated based on the sizes of aggregates obtained by DLS method in the beginning of the experiment (before the adsorption). The results of calculations are presented in the diagram in Figure 5. The following sequence of individual nitrogenous bases adsorbed on the DND surface in water at pH~7.4-7.6 in descending order of DND adsorption activity was obtained:

Cytosine > Adenine > Thymine

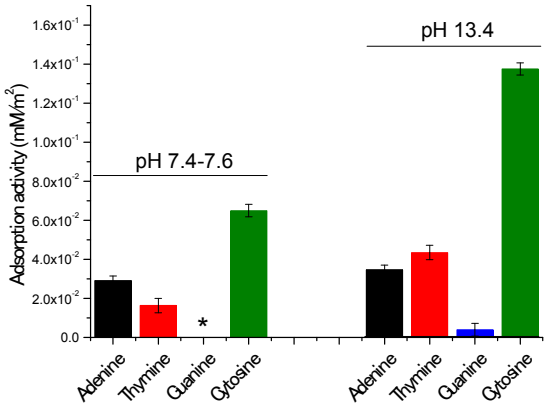

Figure 5. Diagram of DND adsorption activity with regard to individual NBs. * - guanine was not used in the experiments at pH~7.4-7.6

Adsorption of individual DNA nitrogenous bases on the nanodiamonds surface at pH=13.4

To study the interactions of DND-COOH with all DNA NBs including guanine, the aqueous solutions with addition of 0.5 M NaOH of all DNA NBs were prepared at the following concentrations: A – 3 g/L, G – 5 g/L, C – 4 g/L and T – 4 g/L. The initial aqueous suspension of DND-COOH had the same DNA concentration as in the first set of experiments, 2 g/L. Using DLS method it was obtained that the nanodiamond aggregates sizes in the prepared suspensions were 10 nm.

Experiment at pH=13.4 was carried out similarly to experiment with pH 7.4-7.6. Using the calibration dependencies of each NBs marker intensities on its concentration (Figure 3, Figures S1-S3), the concentration of NBs not adsorbed on the DND surface was determined. The measurements of NBs concentrations in the initial mixtures and supernatants demonstrated that

all NBs are adsorbed to a different degree on the nanodiamond surface. The NBs concentrations in supernatant were decreased after adsorption relative to the initial concentrations as follows: A – by 20%, G – by 4%, C – by 57%, T – by 11%.

The adsorption activity of DND with regard to each DNA NB in alkaline medium was calculated. The results of calculations are presented in the diagram in Figure 5. As it can be seen in Figure 5 in alkaline media adsorption activity of all NB**s** on the surface of DND increases in comparison with physiological media, for example, for thymine and cytosine almost in 2 times. Guanine starts to get adsorbed in the alkaline solution. As it is known, at high pH (pH>9-10) amino groups of DNA NBs in water are deprotonated and charged negatively. At the same time, there is a possibility of interactions between negative amino groups of NBs and surface carboxyl groups of DND with an excessive positive charge on the hydrogen atom. These interactions certainly influence on the process of adsorption of NB on DND. It can be assumed that this explains the increase in adsorption activity of DNA NBs on the DND surface at pH=13.4 (see Figure 5).

Thus, the following sequences of individual nitrogenous bases adsorbed on the DND surface in alkaline and water media in descending order of DND adsorption activity were obtained:

$$\text{Cytosine} > \text{Thymine} \geq \text{Adenine} > \text{Guanine (in alkaline medium)} \quad (1)$$

$$\text{Cytosine} > \text{Adenine} > \text{Thymine (in aqueous medium)}$$

Unfortunately, we found neither theoretical nor experimental data on the study of the adsorption of DNA NBs on the surface of nanodiamonds. There are literature data on the study of the adsorption of DNA NBs on the surface of other carbon nanoparticles, namely, carbon nanotubes[33,50-55] and graphene.[38,39,50,53]

Most of the authors in the result of theoretical calculations of binding energy of DNA NBs with the surface of carbon nanotubes[50-53] and graphene[37,39,50,53] obtained the following sequences:

Guanine > Adenine > Thymine > Cytosine (2)

Guanine > Adenine ~ Thymine > Cytosine (2')

The signs > and ~ between A and T correspond to different calculation parameters (different geometry optimization, different chirality of carbon nanotubes[55] etc.).

As results of the calculations of energies of interactions of DNA NBs with carbon nanotubes using such methods as first-principle Hartre-Fock method together with classical force field[33], molecular dynamics[54], density functional reactivity theory based on comprehensive decomposition analysis of stabilization energy[55] the authors[33,54,55] obtained the other sequences :

Thymine > Cytosine > Adenine > Guanine (3), [54]

Guanine > Thymine > Cytosine > Adenine (4), [55]

Adenine >Thymine > Cytosine > Guanine (5), [55]

Guanine > Thymine > Adenine > Cytosine (6), [33]

As can be seen, the sequence of DNA NBs in the rows (2) – (6) varies even for the same carbon materials. The authors of this article did not find any articles devoted to the studies of interaction of nanodiamonds with NBs. Comparing results of our study with the results of studies of molecules adsorption on the other nanocarbons, one can make a conclusion that adsorption of NBs on NDs is different from that on the other nanocarbons. There are known articles in which

the authors noted mismatches between adsorption on the surface of the nanodiamonds with the classical theory of adsorption. For example, in ref.[56] it was found that the same ND may have high adsorption capacity for drug (doxorubicin) and low bonding strength toward it at the same time. The similar conclusion was made by the authors of ref.[57] in the results of research of dyes (propidium iodide) adsorption on NDs surface. Thus, our results are another example of that the process of adsorption on NDs surface is much more complicated and needs further studies to resolve mismatches between classical theory of adsorption and experimental results.

Adsorption of DNA NBs complementary pairs on the detonation nanodiamonds surface.

The similar experiments were carried out to study adsorption of DNA NBs complementary pair (A+T) at pH=7.4-7.6 in aqueous media and (A+T) and (G+C) at pH=13.4 in alkali media on the DND surface.

In water the initial solution of complementary pair (A+T) with the concentrations of A – 1.04 g/L and T – 1.01 g/L was prepared (pH=7.4-7.6). In water with addition of 0.5 M NaOH the initial solutions of complementary pairs (A+T) and (G+C) were prepared with the following concentrations: A – 2 g/L, T – 1.9 g/L, G – 2 g/L, C – 1.5 g/L (pH=13.4). In both experiments these concentrations were chosen to provide equal number of molecules of complementary NBs. Then the solutions of complementary pairs of NBs were mixed with 2 g/L DND aqueous suspension in the ratio 1:1. The study of adsorption of complementary pairs on the DND surface was carried out similarly to the study of the adsorption of individual DNA NBs on the DND surface.

The results of measurement of DNA NBs concentrations after adsorption on nanodiamond surface are presented in Figure 6.

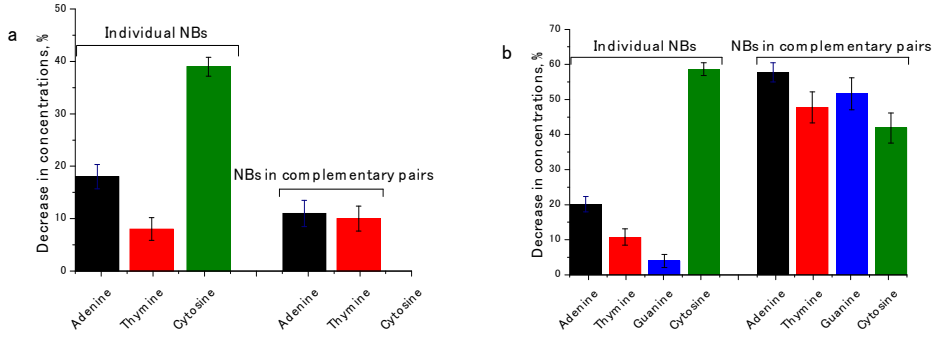

Figure 6. Diagrams of the decrease in the concentration of DNA NBs in supernatants after adsorption of the individual NBs and the NBs complementary pairs on the DND surface during two hours incubation time compared with the initial concentrations before adsorption: a) in aqueous medium (pH=7.4-7.6); b) in alkaline medium (pH=13.4).

From the obtained results it follows that in result of adsorption of NB as a part of complementary pairs on the DND surface the concentration of each NB has decreased relative to the initial as follows: i) A – by 11%, T – by 10% in aqueous medium (pH=7.4-7.6); ii) A – by 58%, G – by 55%, C – by 45%, T – by 50% in alkaline medium (pH =13.4).

Comparative analysis of the obtained experimental results demonstrates that the adsorption properties of individual NBs and NBs, bonded in complementary pairs (A+T) and (C+G), were significantly different (Figure 6). In both experiments, in the case of adsorption of individual DNA NBs larger amount of adenine was adsorbed as compared to thymine. But A and T bonded by hydrogen bonds in a pair are adsorbed on the DND surface approximately equally. A similar situation is observed for the pair (G+C). Guanine in unbounded state is practically not adsorbed on DND surface and cytosine is adsorbed better than the other NBs. In the complementary pair,

however, both guanine and cytosine are adsorbed approximately equally (in comparison with adsorption of the individual NBs). It follows from this that there is a high probability that in the solution of complementary pair C+G cytosine is adsorbed together with guanine on the DND surface. This may mean that the adsorption in solution in which there is pair, cytosine is adsorbed only with guanine, and adenine with thymine, i.e, the complementary pairs are not destroyed. Thus, the obtained results indicate that during adsorption of the complementary pairs on the DND surface there is no break of hydrogen bonds between the components of the complementary pair.

The difference in the amount of adsorbed pairs in aqueous and alkaline media is explained by the change in pH of the medium. The authors[58,59] also observed that with increasing pH the adsorption of doxorubicin[58] and some organic molecules (phenol, aniline, o-aminophenol, nitrobenzene etc.)[59] on the surface of carboxylated DND is more active. Table S1 contains numerical data of the performed calculations of the change of the concentration after adsorption.

IR absorption spectroscopy.

Following experiments on adsorption of individual DNA NBs and their complementary pairs on DND surface the IR absorption spectra of all extracted sediments – DND with adsorbed NBs – were obtained. As an example, Figure 7 illustrates IR spectra of sediments DND-COOH, complementary pair (A+T) and complex (DND-COOH)+(A+T).

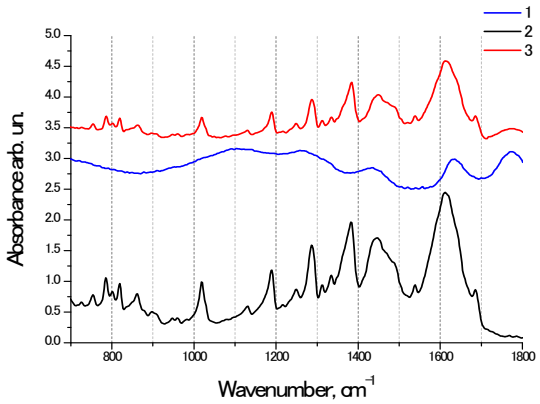

Figure 7. The IR absorption experimental spectra of DND-COOH powder (1), complementary pair (A+T) (2) and sediment (DND-COOH)+(A+T) after adsorption A+T on the DND surface (3). Spectra are taken for dried samples.

The analysis of obtained IR spectra shows that in the IR spectra of adsorbents with adsorbates there are no new bands in comparison with the spectra of DND-COOH and complementary pairs (A+T) and (G+C). Therefore, NBs and their pairs interact with the carboxylated DND surface by means of physical adsorption.

Molecular Modeling

Interactions of individual DNA NBs and their complementary pairs with diamond-like nanoparticles were analyzed using DFT molecular modelling.

As a model of nanodiamond with surface carboxylic groups 1,3,5,7-adamantanecarbonyl acid was used. The structure of 1,3,5,7- adamantanecarbonyl acid is illustrated in Figure 8a, while calculated and experimental IR spectrum of carboxylated nanodiamond are provided in Figure 8b.

In the calculated IR spectrum five characteristic areas can be distinguished: peaks in the region from 1000 to 1200 cm^{-1} can be assigned to the stretching vibrations of C-O bonds in carboxylic groups, stretching vibrations of C-C bonds and bending vibrations of C-H bonds; the region from 1780 to 1800 cm^{-1} corresponds to the stretching vibrations of C=O bonds in carboxylic groups; two regions - from 2915 to 2950 cm^{-1} and from 2980 to 2995 cm^{-1} –correspond to the stretching symmetric and antisymmetric vibrations of CH bonds, respectively; the region near 3523 cm^{-1} corresponds to the stretching vibrations of O-H bonds in carboxylic groups. The wavenumbers of the most intense peaks in the stated regions are 1144, 1795, 2917, 2994 and 3523 cm^{-1}.

The chosen characteristic regions in the obtained IR spectrum are in a good agreement with the corresponding regions in the experimental IR spectrum of nanodiamond functionalized by carboxylic groups (Figure 8b). Based on these results, 1,3,5,7-adamantanecarbonyl acid can be considered as a model of carboxylated nanodiamond to provide qualitative assessments of formed bonds with NBs and analyze their properties.

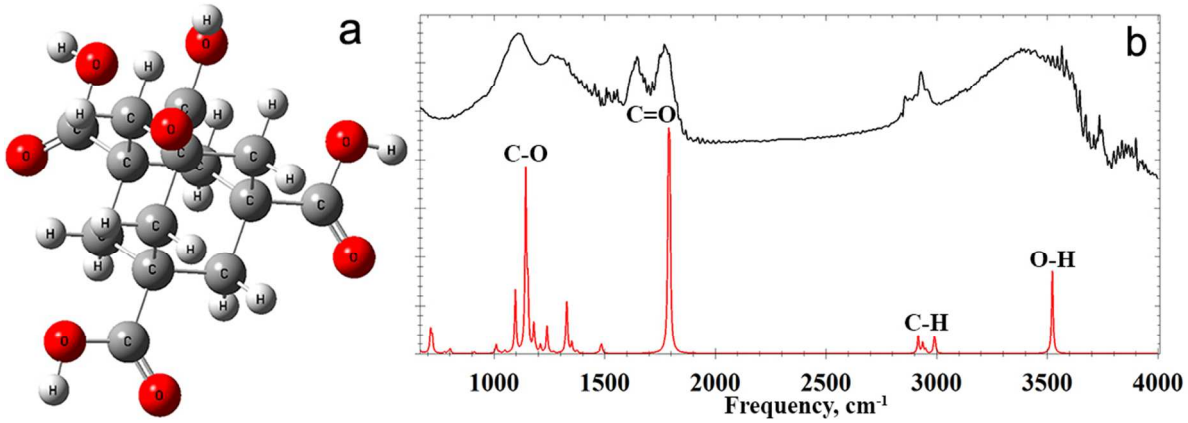

Figure 8. The structure of 1,3,5,7-adamantanecarbonyl acid (a) and calculated (lower) and experimental (upper) IR spectra of nanodiamond functionalized by carboxylic groups (b).

Below in the description of theoretical calculations we will continue to use the designations DND and DND-COOH assuming that 1,3,5,7-adamantanecarbonyl acid is used as the calculation model.

The optimized structures of complementary pair (A+T), DND-COOH and (A+T)+(DND-COOH) complex surrounded by water molecules (Figure 9 a-d) were calculated. The possibility of attachment of the complementary pair to the 1,3,5,7-adamantanecarbonyl acid was studied in two configurations – via thymine and via adenine. Within the complimentary pair (A+T), there are two hydrogen bonds formed.[60] Same configuration of the complementary pair (A+T) as in ref.[60] was formed as a result of our calculations (bonds 1 and 2, Figure 9 a,c,d) taking into account water molecules surrounding the pair (A+T). For the complex of the complementary pair (A+T) with DND-COOH surrounded by 6 water molecules our calculations demonstrated that the pair (A+T) can be attached to the carboxylated DND both via thymine and via adenine. In this case two hydrogen bonds are formed between the complementary pair and DND: 3c and 4c when the attachment occurs via thymine (Figure 9c), 8d and 9d when the attachment occurs via adenine (Figure 9d) while both hydrogen bonds between adenine and thymine are retained (bonds 1 and 2 (Figure 9 a,c,d)).

Thus, the process of the complementary pair (A+T) adsorption on the surface of carboxylated DND surrounded by 6 water molecules was numerically modelled. On the basis of the calculated IR absorption spectra of a separate pair (A+T) and the molecular complex (A+T)+(DND-COOH) surrounded by 6 water molecules the analysis of changes in geometric parameters of hydrogen bonds between molecules during formation of the complex (A+T)+(DND-COOH) was carried out. The results of calculations are demonstrated in Table 1. The notations of hydrogen bonds correspond to the numeration of bonds shown in the Figure 9.

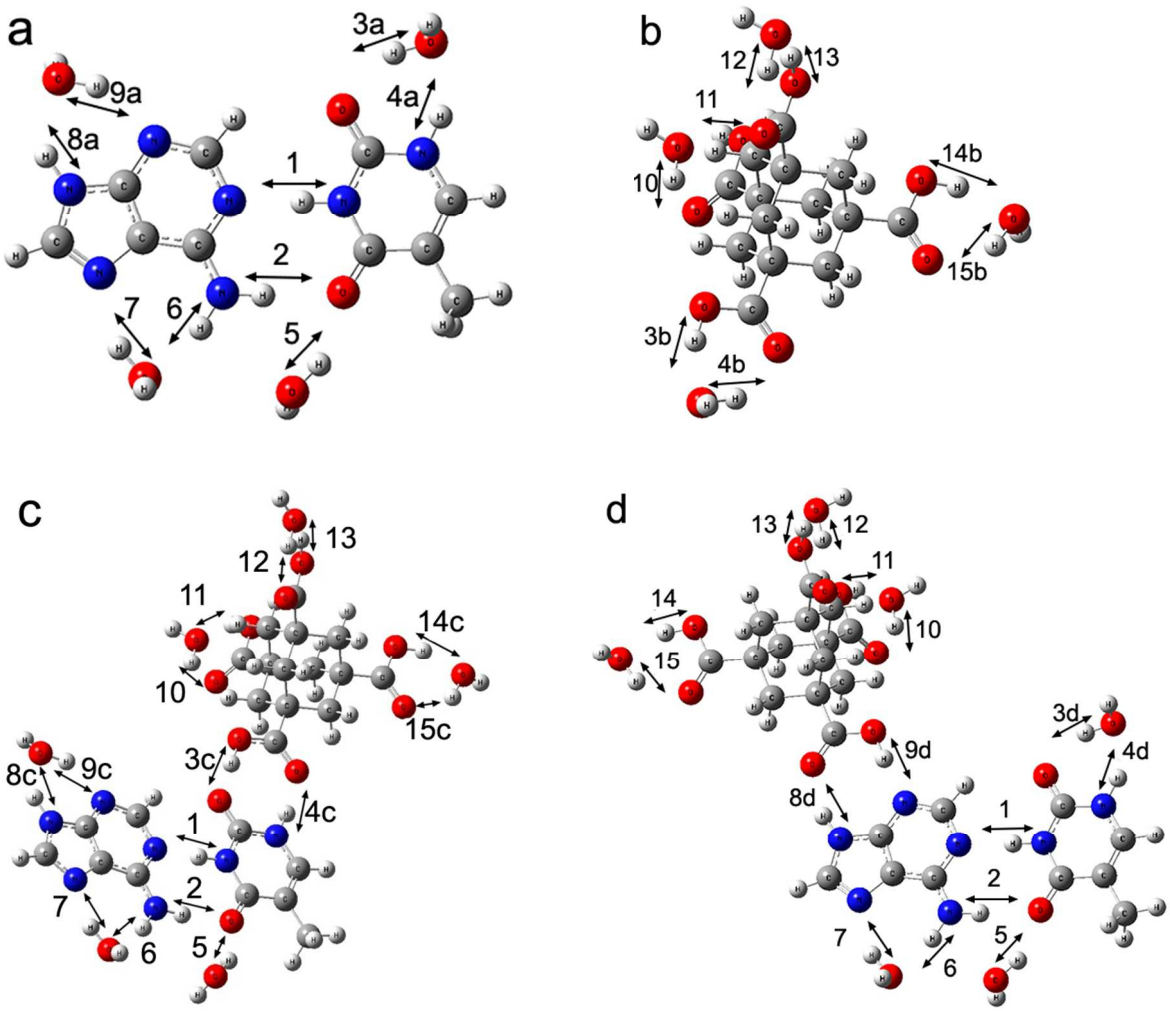

Figure 9. The optimized structures of (a) complementary pair A+T; (b) DND-COOH; (c) the molecular complex (A+T)+(DND-COOH) (for the attachment of the complementary pair via thymine); and (d) the molecular complex (A+T)+(DND-COOH) (for the attachment of the complementary pair via adenine) surrounded by water molecules.

Table 1. The calculated parameters (lengths) of hydrogen bonds between the molecules in the (A+T) (a), DND-COOH (b) and complex (A+T)+(DND-COOH) (c,d) surrounded by 6 water molecules (see Figure 9 for the bonds notation).

Number of bond	Bond	a	b	c	d
		Length, A	Length, A	Length, A	Length, A
1	H···N	1.83		1.83	1.84
2	H···O	2.01		2.01	2.02
3	H···O	1.91	1.74	1.68	1.91
4	H···O	1.87	1.92	1.77	1.88
5	H···O	1.97		1.97	1.97
6	H···O	1.87		1.88	1.87
7	H···N	1.93		1.92	1.92
8	H···O	1.95		1.95	1.84
9	H···N	1.98		1.98	1.73
10	H···O		1.93	1.94	1.93
11	H···O		1.73	1.73	1.74
12	H···O		1.93	1.94	1.93
13	H···O		1.73	1.73	1.73
14	H···O		1.73	1.73	1.73
15	H···O		1.93	1.93	1.93

Energies of hydrogen bonds (1,2), (3,4), (8,9) and (14,15) were calculated for starting configurations of (A+T) pair surrounded by water molecules, DND-COOH surrounded by water molecules and for the complementary pairs adsorbed on the DND surface (Table S2). Energy of bonds was calculated using Iogansen's formula:[61-63] $-\Delta H = 0.3 \cdot \sqrt{\Delta\nu - 40}$, where Δν is the change in the frequency of stretching vibrations of a donor group in the formation of hydrogen

bonds between the group and water molecule (the cases a and b in Figure 9) or during the process of interactions of the (A+T) pair and the DND-COOH (the cases c and d in Figure 9).

The analysis of the calculated parameters of hydrogen bonds in the optimized configurations has demonstrated that the complementary pair (A+T) in the presence of water molecules is adsorbed on the DND-COOH surface in two ways. (i) In one path the hydrogen bonds can be formed between C-O and N-H molecular groups of thymine and O-H and C-O end groups of DND carboxylic groups, respectively (bonds 3c and 4c, Figure 9c). In such attachment of (A+T) via thymine, hydrogen bond 3c is the strongest one. The bond 4c is also strengthened in comparison with hydrogen bond 4a. In another path the hydrogen bonds can be formed between N-H and C-N molecular groups of adenine and C-O and O-H end groups of DND carboxylic groups, respectively (bonds 8d and 9d, Figure 9d). In the attachment of A+T via adenine, hydrogen bond 9d is significantly strengthened. The bond 8d is slightly strengthened in comparison with hydrogen bond 8a. In this case, the strength of hydrogen bond 9d is about 17% greater than that of the bond 3c. Thus, in the configurations (A+T)+(DND-COOH), the attachment of the complementary pair to DND via adenine is stronger.

The calculations also demonstrated that during the adsorption of pair (A+T) on the DND-COOH surface in the presence of water molecules the hydrogen bonds between adenine and thymine (the bonds 1 and 2, Figure 9a,c,d) do not collapse, however the parameters of the bonds 1 and 2 change. In the case of the attachment of (A+T) to DND via thymine the insignificant strengthening of the bond 1c in comparison with the strength of this bond in non-adsorbed pair (A+T) (1a) occurs. In the case of the attachment of (A+T) to DND via adenine the hydrogen bond 1 weakens (by 2.4%) in comparison with the hydrogen bond 1a. The hydrogen bond 2 in both cases remains practically unchanged.

The comparative analysis of the strength of the hydrogen bonds 3a and 3d, 4d and 4a, and 8a and 8b, 9a and 9d shows that in the case of the attachment of (A+T) to DND via thymine the hydrogen bonds of adenine with surrounding water molecules are not changed. Similar, in the case of the attachment of (A+T) to DND via adenine the hydrogen bonds of thymine with surrounding water molecules are not changed.

The comparison of the strength of the hydrogen bonds 14 and 15 between the DND carboxylic groups and surrounding water molecules shows that they are practically unchanged in both ways of the attachment of (A+T) to DND.

In the complex adsorbate+adsorbent the hydrogen bonds between DND and adenine (8d and 9d) or thymine (3b and 4b) are stronger than the hydrogen bonds between non-absorbed pair (A+T) and water molecules (3a and 4a, 8a and 9a, and 5,6,7), demonstrating thermodynamic stability of the bonds formed between DND-COOH and the (A+T) complementary pair.

Conclusion

As the result of experimental study of interactions of individual DNA NBs and their complementary pairs with the surface of carboxylated DND in water suspensions, it was found that DND-COOH demonstrated substantial difference in the adsorption activity with respect to individual NBs, and nearly the same adsorption activity with respect to NBs bonded in complementary pairs.

The following sequences have been obtained for the adsorption activity of DND with regard to each DNA NBs on DND surface in decreasing order:

Cytosine > Thymine ≥ Adenine > Guanine (in alkaline medium)

Cytosine > Adenine > Thymine (in aqueous medium)

It was found that NBs were adsorbed on the DND surface nearly equally when they formed complementary pairs. This may mean that NBs complementary pairs are preserved during adsorption.

Analysis of the obtained IR spectra of individual NBs, of their complementary pairs, DND+COOH and DND with the adsorbed complementary pairs (A+T) and (C+G) have demonstrated that NBs and their complementary pairs interact with the surface of carboxylated DND via physical adsorption.

Basing on molecular modeling using the method of the density functional theory, the interactions of the complementary pairs of DNA NBs and diamond-like nanoparticles were analyzed. The theoretical calculations confirmed the obtained experimental results, namely:

1. The complementary pairs are adsorbed on the DND surface functionalized by carboxylic groups by formation of the hydrogen bonds, i.e. via physical adsorption.

2. During the adsorption of the complementary pairs on the DND surface, no break of the hydrogen bonds between the components of NBs pair occurs.

Supporting Information Description

Supporting information file contains four Figures, two Tables (Table S1 - Amount of NBs adsorbed on NDs and DND adsorption activity at different pH, Table S2 - The calculated values

of the energy of the hydrogen bonds (3,4), (8,9) and (14,15)), detailed plan of the experiment and calibration curves.

Acknowledgements

This study has been performed at the expense of the grant of Russian Science Foundation (project No 17-12-01481).

References

1. Stewart, M. P.; Sharei, A.; Ding, X.; Sahay, G.; Langer, R.; Jensen, K. F. In Vitro and Ex Vivo Strategies for Intracellular Delivery. *Nature* **2016**, *538*, 183-192.

2. Juliano, R. L. The Delivery of Therapeutic Oligonucleotides. *Nucleic Acids Res.* **2016**, *44(14)*, 6518-6548.

3. Zhao, J.; Feng, S.-S. Nanocarriers for Delivery of siRNA and Co-delivery of siRNA and Other Therapeutic Agents. *Nanomedicine* **2015**, *10*, 2199-2228.

4. Massadeh, S.; Al-Aamery, M.; Bawazeer, S.; AlAhmad, O.; AlSubai, R.; Barker, S.; Craig, D. Nano-materials for Gene Therapy: An Efficient Way in Overcoming Challenges of Gene Delivery. *Journal of Biosensors & Bioelectronics* **2016**, *7(195)*, 1-12.

5. Rajabi, M.; Srinivasan, M.; Mousa, S. A. *Nanobiomaterials in Drug Delivery. In Nanobiomaterials in Drug Delivery: Applications of Nanobiomaterials*; Elsevier Amsterdam: 2016.

6. Li, J.; Xue, S.; Mao, Z.-W. Nanoparticle Delivery Systems for siRNA-based Therapeutics. *J. Mater. Chem. B* **2016**, *41*, 6620-6639.

7. Prabhakar, N.; Nareoja, T.; von Haartman, E.; Sen Karaman, D.; Burikov, S. A.; Dolenko, T. A.; Jaikishan, S.; Mamaeva, V.; Hanninen, P. E.; Vlasov, et al. Functionalization of Graphene Oxide Nanostructures Improves Photoluminescence and Facilitates their Use as Optical Probes in Preclinical Imaging. *Nanoscale* **2015**, *7*, 10410-10420.

8. Rosenholm, J. M.; Vlasov, I. I.; Burikov, S. A.; Dolenko, T. A.; Shenderova, O.A. Nanodiamond-Based Composite Structures for Biomedical Imaging and Drug Delivery (Review). *J. Nanosci. Nanotechnol.* **2015**, *15*, 959-971.

9. Prabhakar, N.; Nareoja, T.; von Haartman, E.; Karaman, D. S.; Jiang, H.; Koho, S.; Dolenko, T.; Hanninen, P.; Vlasov, D. I.; Ralchenko, et al. Core-shell Designs of Photoluminescent Nanodiamonds with Porous Silica Coatings for Bioimaging and Drug Delivery II: Application. *Nanoscale* **2013**, *5(9)*, 3713-3722.

10. Mochalin, V.; Shenderova, O.; Ho, D.; Gogotsi, Y. The Properties and Applications of Nanodiamonds. *Nat. Nanotechnol.* **2011**, *7(1)*, 11-23.

11. Turcheniuk, K.; Mochalin, V. N. Biomedical Applications of Nanodiamond (Review). *Nat. Nanotechnol.* **2017**, *28*, 252001-252028

12. Schrand, A. M.; Hens, S. A.; Shenderova, O. A. Nanodiamond Particles: Properties and Perspectives for Bioapplications. *Crit. Rev. Solid State Mater. Sci*. **2009**, *34*, 18-74.

13. Shenderova, O.; McGuire, G. E. Science and Engineering of Nanodiamond Particle Surfaces for Biological Applications. *Biointerphases* **2015**, *030802*, 1-24.

14. Zhang, X.-Q.; Chen, M.; Lam, R.; Xu, X.; Osawa, E.; Ho, D. Polymer-functionalized Nanodiamond Platforms as Vehicles for Gene Delivery. *ACS Nano* **2009**, *3*, 2609-2616.

15. Kaur, R.; Chitanda, J. M.; Michel, D.; Maley, J.; Borondics, F.; Yang, P.; Verrall, R. E.; Badea, I. Lysine-functionalized Nanodiamonds: Synthesis, Physiochemical Characterization, and Nucleic Acid Binding Studies. *Int. J. Nanomed.* **2012**, *7*, 3851–3866.

16. Petrakova, V.; Benson, V.; Buncek, M.; Fiserova, A.; Ledvina, M.; Stursa, J.; Cigler, P.; Nesladek, M. Imaging of Transfection and Intracellular Release of Intact, Non-labeled DNA Using Fluorescent Nanodiamonds. *Nanoscale* **2016**, *8*, 12002-12012.

17. Grichko V.; Shenderova O. *Ultrananocrystalline Diamond: Synthesis, Properties and Applications*; William-Andrew Publisher, 2006.

18. Grichko, V.; Grishko, V.; Shenderova, O. Nanodiamond Bullets and Their Biological Targets. *Nanobiotechnology*, **2007**, *2*, 37-42.

19. Kim, H.; Man, H. B.; Saha, B.; Kopacz, A. M.; Lee, O.-S.; Schatz, G. C.; Ho, D.; Liu, W. K. Multiscale Simulation as a Framework for the Enhanced Design of Nanodiamond-polyethylenimine-based Gene Delivery. *J. Phys. Chem. Lett.* **2012**, *3*, 3791-3797.

20. Chen, M.; Zhang, X.-Q.; Man, H. B.; Lam, R.; Chow, E. K.; Ho, D. Nanodiamond Vectors Functionalized with Polyethylenimine for siRNA Delivery. *J. Phys. Chem. Lett.* **2010**, *1*, 3167-3171.

21. Alhaddad, A.; Adam, M. P.; Botsoa, J.; Dantelle, G.; Perruchas, S.; Gacoin, T.; Mansuy, C.; Lavielle, S.; Malvy, C.; Treussart, F. Nanodiamond as a Vector for siRNA Delivery to Ewing Sarcoma Cells. *Small* **2011**, *7*, 3087-3095.

22. Alhaddad, A.; Durieu, C.; Dantelle, G.; Le Cam, E.; Malvy, C.; Treussart, F.; Bertrand, J.-R. Influence of the Internalization Pathway on the Efficacy of siRNA Delivery by Cationic Fluorescent Nanodiamonds in the Ewing Sarcoma Cell Model. *PLoS One* **2012**, *7*, e52207.

23. Cao, M.; Deng, X.; Su, S.; Zhang, F.; Xiao, X.; Hu, Q.; Fu, Y.; Yang, B. B.; Wu, Y.; Sheng, W. Protamine Sulfate–nanodiamond Hybrid Nanoparticles as a Vector for MiR-203 Restoration in Esophageal Carcinoma Cells. *Nanoscale* **2013**, *5*, 12120-12125.

24. Purtov, K. V.; Burakova, L. P.; Puzyr, A. P.; Bondar, V.S. The Interaction of Linear and Ring Forms of DNA Molecules with Nanodiamonds Synthesized by Detonation. *Nanotechnology* **2008**, *19*, 325101.

25. Ushizawa, K.; Sato, Y.; Mitsumori, T.; Machinami, T.; Ueda, T.; Ando, T. Covalent Immobilization of DNA on Diamond and its Verification by Diffuse Reflectance Infrared Spectroscopy. *Chem. Phys. Lett.* **2002**, *351*, 105-108.

26. Yang, J. H.; Song, K. S.; Zhang, G. J.; Degawa, M.; Sasaki, Y.; Ohdomari, I.; Kawarada, H. Characterization of DNA Hybridization on Partially Aminated Diamond by Aromatic Compounds. *Langmuir* **2006**, *22(26)*, 11245-11250.

27. Song, K. S.; Zhang, G. J.; Nakamura, Y.; Furukawa, K.; Hiraki, T.; Yang, J. H.; Funatsu, T.; Ohdomari I.; Kawarada H. Label-free DNA Sensors Using Ultrasensitive Diamond Field-Effect Transistors in Solution. *Phys. Rev. E* **2006**, *74(4)*, 0419191

28. Pohl, A.; Joch, S.; Michael, J.; Boschke, E.; Quenzel, P.; Schreiber, J.; Lapina, V.; Opitz, J. Testing Possibilities for Establishing Nanodiamond-DNA-conjugates. *Clinical and Biomedical Spectroscopy and Imaging II SPIE; Opt Soc Amer–SPIE* **2011**, *8087*, 80871T.

29. Gaillard, C.; Girard, H. A.; Falck, C.; Paget, V.; Simic, V.; Ugolin, N.; Bergonzo, P.; Chevillard, S.; Arnault, J.-C. Peptide Nucleic Acid–nanodiamonds: Covalent and Stable Conjugates for DNA Targeting. *RSC Adv.*, **2014**, *4*, 3566–3572.

30. Zhang, T.; Neumann, A.; Lindlau, J.; Wu, Y.; Pramanik, G.; Naydenov, B.; Jelezko, F.; Schuder, F.; Huber, S.; Huber, et al. DNA-Based Self-Assembly of Fluorescent Nanodiamonds. *J. Am. Chem. Soc.* **2015**, *137*, 9776−9779.

31. Bokarev, A. N.; Plastun, I. L.; Agendeeva, K. E. Infuence of Hydrogen Bonding on IR Spectra and Structure of Molecular Complex of Diamond-like Nanoparticles and DANN Nucleobases. *Izvestiya SGU. Novaya seriya. Seria fizika*. **2016**, *16(4)*, 218-227. (in Russian)

32. Stepanian, S. G.; Karachevtsev, M. V.; Glamazda, A. Yu.; Karachevtsev, V. A.; Adamowicz, L. Raman Spectroscopy and Theoretical Characterization of Nanohybrids of Porphyrins with Carbon Nanotubes. *J. Phys. Chem. A* **2009**, *113(15)*, 3621–3629.

33. Das, A.; Sood, A. K.; Maiti, P. K.; Das, M.; Varadarajan, R.; Rao, C. N. R. Binding of Nucleobases With Single-walled Carbon Nanotubes: Theory and Experiment. *Chem. Phys. Lett.* **2008**, *453(4-6)*, 266–273.

34. Liu, B.; Salgado, S.; Maheshwari, V.; Liu, J. DNA Adsorbed on Graphene and Graphene Oxide: Fundamental Interactions, Desorption and Applications. *Curr. Opin. Colloid Interface Sci.* **2016**, *26*, 41-49.

35. Sowerby, S. J.; Cohn, C. A.; Heckl, W. M.; Holm, N. G. Differential Adsorption of Nucleic Acid Bases: Relevance to the Origin of Life. *PNAS*. **2001**, *98(3)*, 820–822.

36. Gowtham, S.; Scheicher, R. H.; Ahuja, R.; Pandey, R.; Karna, S. P. Physisorption of Nucleobases on Graphene: Density-functional Calculations. *Phys. Rev. B: Condens. Matter* **2007**, *76(3)*, 2–5.

37. Varghese, N.; Mogera, U.; Govindaraj, A.; Das, A.; Maiti, P. K.; Sood, A. K.; Rao, C. N. Binding of DNA Nucleobases and Nucleosides with Graphene. *ChemPhysChem* **2009**, *10(1)*, 206–210.

38. Antony, J.; Grimme, S. Structures and Interaction Energies of Stacked Graphene–nucleobase Complexes. *Phys Chem Chem Phys*. **2008**, *10*, 2722–2729

39. Sponer, J.; Riley, K. E.; Hobza, P. Structures and Interaction Energies of Stacked Graphene–nucleobase Complexes. *Phys. Chem. Chem. Phys.* **2008**, *10*, 2581–2583.

40. Petit, T.; Puskar, L.; Dolenko, T.; Choudhury, S.; Ritter, E.; Burikov, S.; Laptinskiy, K.; Brzustowski, Q.; Schade, U.; Yuzawa, H., et al. Unusual Water Hydrogen Bond Network around Hydrogenated Nanodiamonds *J. Phys. Chem. C* **2017**, *121(9)*, 5185–5194.

41. Dolenko, T. A.; Burikov, S. A.; Rosenholm, J. M.; Shenderova, O. A.; Vlasov, I. I. Diamond-water Coupling Effects in Raman and Photoluminescence of Nanodiamond Colloidal Suspensions. *J. Phys. Chem. C* **2012**, *116*, 24314-24319.

42. Dolenko, T. A.; Burikov, S. A.; Laptinskiy, K. A.; Rosenholm, J. M.; Shenderova, O. A.; Vlasov, I.I. Evidence of Carbon Nanoparticle–Solvent Molecule Interactions in Raman and Fluorescence Spectra. *Phys. Status Solidi A* **2015**, *212(11)*, 2512-2518.

43. Vervald, A. M.; Burikov, S. A.; Shenderova, O. A.; Nunn, N.; Podkopaev, D. O.; Vlasov, I.I.; Dolenko, T.A. Relationship Between Fluorescent and Vibronic Properties of Detonation Nanodiamonds and Strength of Hydrogen Bonds in Suspensions *J. Phys. Chem. C*, **2016**, *120(34)*, 19375-19383.

44. Shenderova, O.; Panich, A. M.; Moseenkov, S.; Hens, S. C.; Kuznetsov, V.; Vieth, H.-M. Hydroxylated Detonation Nanodiamond: FTIR, XPS, and NMR Studies. *J. Phys. Chem. C* **2011**, *115*, 19005-19011.

45. Saenger, W. *Why Study Nucleotide and Nucleic Acid Structure;* Springer, New York, NY, 1984.

46. Dolenko, T. A.; Burikov, S. A.; Laptinskiy, K. A.; Moskovtsev, A. A.; Mesitov, M. V.; Kubatiev, A. A. Improvement of Fidelity of Molecular DNA Computing Using Laser Spectroscopy. *Laser Phys.* **2015**, *25(3)*, 035202 10pp.

47. Kohn, W. The Electronic Structure of Matter: Wave Functions and Density Functionals. *Physics-Uspekhi (Advances in Physical Sciences)* **2002**, *172(3)*, 336-348.

48. Pople, J. Quantum Chemical Models. *Phys. Usp.* **2002**, *172(3)*, 349-356.

49. Frisch, M. J.; Trucks, G. W.; Schlegel, H. B.; Scuseria, G. E.; Robb, M. A.; Cheeseman, J. R.; Scalmani, G.; Barone, V.; Mennucci, B.; Petersson, G. A., et al. Gaussian 09, Revision A.1; Gaussian, Inc.: Wallingford, CT, 2009.

50. Ramraj, A.; Hillier, I. H.; Vincent, M. A.; Burton, N. A. Assessment of Approximate Quantum Chemical Methods for Calculating the Interaction Energy of Nucleic Acid Bases with Graphene and Carbon Nanotubes. *Chem. Phys. Lett.* **2010**, *484*, 295–298.

51. Yamazaki, T.; Fenniri, H. Imaging Carbon Nanotube Interaction with Nucleobases in Water Using the Statistical Mechanical Theory of Molecular Liquids. *J. Phys. Chem. C* **2012**, *116(28)*, 15087–15092.

52. Lv, W. The Adsorption of DNA Bases on Neutral and Charged (8, 8) Carbon-nanotubes. *Chem. Phys. Lett.* **2011**, *514(4–6)*, 311–316.

53. Umadevi, D.; Sastry, G. N. Quantum Mechanical Study of Physisorption of Nucleobases on Carbon Materials: Graphene Versus Carbon Nanotubes. *J. Phys. Chem. Lett.* **2011**, *2*, 1572–1576.

54. Frischknecht, A. L.; Martin, M. G. Simulation of the Adsorption of Nucleotide Monophosphates on Carbon Nanotubes in Aqueous Solution. *J. Phys. Chem. C* **2008**, *112*, 6271–6278.

55. Sarmah, A.; Roy, R. K. Understanding the Interaction of Nucleobases with Chiral Semiconducting Single- walled Carbon Nanotubes: An Alternative Theoretical Approach Based on Density Functional Reactivity Theory. *J. Phys. Chem. C* **2013**, *117*, 21539–21550.

56. Mochalin, V.; Pentecost, A.; Li, X.-M.; Neitzel, I.; Nelson, M.; Wei, C.; He, T.; Guo, F.; Gogotsi, Yu. Adsorption of Drugs on Nanodiamond: Toward Development of a Drug Delivery Platform. *Mol. Pharmaceutics* **2013**, *10(10)*, 3728–3735.

57. Gibson, N.; Luo, T.-J.; Shenderova, O.; Koscheev, A.; Brenner, D. Electrostatically Mediated Adsorption by Nanodiamond and Nanocarbon Particles. *J. Nanopart. Res.* **2012**, *14 (3)*, 1−12.

58. Yan, J.; Guo, Y.; Altawashi, A.; Moosa, B.; Lecommandouxc, S.; Khashab, N. M. Experimental and Theoretical Evaluation of Nanodiamonds as pH Triggered Drug Carriers. *New J. Chem.* **2012**, *36(7)*, 1479-1484.

59. Lanin, S. N.; Rychkova, S. A.; Vinogradov, A. E.; Lanina, K. S.; Obrezkov, O. N.; Nesterenko, P. N. Modification of the Surface Chemistry of Microdispersed Sintered Detonation Nanodiamonds and its Effect on the Adsorption Properties. *Adsorption* **2017**, *23*, 639-650.

60. Ten, G. N.; Nechaev, V. V.; Pankratov, A. N.;.Berezin, V. I; Baranov, V. I. Effect of Hydrogen Bonding on the Structure and Vibrational Spectra of the Complementary Pairs of Nucleic Acid Bases. II. Adenine-thymine. *J. Struct. Chem.* **2010**, *51(5)*, 854-861.

61. Iogansen, A.V. Direct Proportionality of the Hydrogen Bonding Energy and the Intensification of the Stretching ν(XH) Vibration in Infrared Spectra. *Spectrochim. Acta, Part A* **1999**, *55(7)*, 1585-1612.

62. Babkov, L. M.; Puchkovskaya, G. A.; Makarenko, S. P.; Gavrilko T.A. *IR Spectroscopy of Molecular Crystals with Hydrogen Bonds;* Naukova Dumka: AS UkrSSR Kiev, 1989.

63. Babkov, L. M.; Baran, J.; Davydova, N. A.; Uspenskiy, K. E. Modeling of the Structure and Vibrational Spectra of 2-biphenylmethanol Using B3LYP Method. *J. Mol. Struct.* **2006**, *792-793*, 68-72.

Table of Contents (TOC) Image